Journal of Engineering Science and Technology
Vol. 15, No. 3 (2020) 2023 - 2039

ENHANCEMENT OF MAGNETIC RESONANCE IMAGES THROUGH PIECEWISE LINEAR HISTOGRAM EQUALIZATION

WAMEEDH RIYADH ABDUL-ADHEEM

Department of Electrical Power Engineering Techniques,
Al-Mamoun University College, Iraq
E-mail: wameedh.r.abduladheem@almamonuc.edu.iq

Abstract

One of the advanced techniques in medical imaging is Magnetic resonance imaging (MRI) that provides deep knowledge of the soft tissue for human anatomy. The enhancement operation of such images helps the doctor of medicine to analyze and act toward several diseases. These operations are utilized using transformation functions, which are constructed automatically using a technique called Conventional Histogram Equalization (CHE). The CHE tends to present unusual artifacts and abnormal enhancement because of extreme compensation of the light level intensities. In this paper, an algorithm called piecewise linear histogram equalization (PLHE) is presented. The proposed algorithm is an extension of CHE that is simple, piecewise linear, and supports a single parameter to control the enhancement process. Two quantitative measures are selected, which are information entropy and sharpness, to show the visual performance improvement of the proposed algorithm. A comparison of the CHE and proposed algorithm demonstrates the development in the visual performance for the latter method.

Keywords: Histogram equalization, Image enhancement, Magnetic resonance imaging.

1. Introduction

An enhancement technique is a process of improving an image so that the result is most suitable for a particular purpose [1]. The enhancement technique should be selected based on the problems and properties of the image because each situation may need a different technique. For the present study, the enhancement technique fall under the category of spatial domain methods. In medical images captured by various equipment, obtaining a large dynamic range increases the likelihood of accuracy, which in turn increases the speed of recovery [2].

Several early suggested algorithms for enhancing images that applied for various applications are summered here. In [3], an enhancement algorithm was suggested for a hyperspectral image resolution based on spectral unmixing. In [4], an innovative image enhancement algorithm for a wide-angle lens camera was suggested based on both space-varying interpolation kernels and local self-similarity. In [5], a novel algorithm for 3-D segmentation was presented based on late gadolinium enhancement magnetic resonance imaging that increases visualization of cardiac left atrium fibrosis. In [6], an innovative denoising algorithm was suggested based on the Curvelet transform. In [7], an enhancement method for remote sensing images was suggested using the regularized-histogram equalization and the discrete cosine transform. In [8], a framework was indicated for both quality enhancement and antiforensics of median filtered images. In [9], an iterative registration algorithm was proposed for integrating multiple optoacoustic are combined into one high-resolution image.

In [10], active contour models were suggested for improving the accuracy of the image reconstruction routines. In [11], a new contrast enhancement algorithm was suggested based on the maximization of the tone-preserving entropy. In [12], a generic training strategy was proposed through a new regularisation model. In [13], an adaptive image enhancement method was suggested based fraction-power transformation. Recently, two medical image enhancement techniques was suggested. The first method, which is given in [14], utilizes stationary wavelet transform and double density wavelet transforms to enhance the contrast and edge for different tissues. The second technique was developed using frequency band broadening and neural networks to improve the resolution of the image being processed, as described in [15].

In this paper, a modification of Conventional Histogram Equalization (CHE) is proposed to improve the visual performance of the CHE method. The resulting image of the CHE method has a considerable difference in the mean light brightness than the original image to be enhanced. A single-point transformation is generated based on the value of a suggested parameter, which is used to threshold the histogram of the image to be enhanced. The outcome transform is simple and piecewise linear. Thus, the proposed algorithm is called Piecewise Linear Histogram Equalization (PLHE),which provides uniformly spread of the histogram components over the grayscale range.

This paper is organized as follows: Section 2 describes the spatial domain techniques such as histogram equalization. The proposed algorithm is described in section 3. The numerical examples and numerical simulations are presented in Sections 4 and 5, respectively. Finally, the conclusion is provided in Section 6.

2. Theoretical Background

2.1. Spatial domain techniques

The collection of pixels in an image is a spatial domain. Applications of specific operators on these pixels are called spatial domain techniques. The basic function used in spatial domain enhancement is [16, 17]

$$I_T(\cdot) = F[I(\cdot)] \tag{1}$$

with $I(x, y)$ being the image to be processed, $I_T(x, y)$ representing the processed image, and $F(.)$ denoting the process operator. The operator F is applied over a small region around (x, y). Usually, this region is defined as a rectangular area with its center at point (x, y). This processing model is given in Eq. (1) can be simplified to a model called point processing, which is defined as [16]:

$$v = F(u) \tag{2}$$

where u and v represent a single point in the input and output images at a spatial location (x, y), respectively.

2.2. Contrast stretching

Sensors used in image processing can cause low contrast for various reasons, such as unsuitable settings for the image capture process or inappropriate lighting in the external environment. As shown in Fig. 1, obtaining a suitable operator for spreading image intensities is called contrast stretching. Such an operation has an essential effect on the redistribution of light intensity and can help address the problems that have been discussed previously [18].

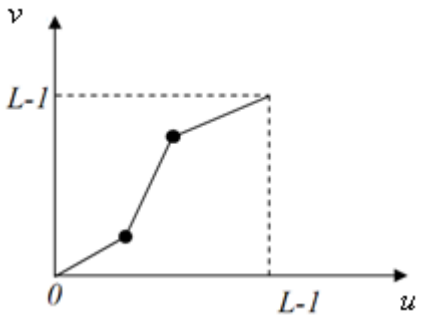

Fig. 1. Contrast stretching transformation.

2.3. Histogram Equalization

In an image, a gray level $u_k \in [0, L-1]$ has an occurrence probability $p(u_k)$, which is called image histogram and expressed as [19]:

$$p(u_k) = \frac{n_k}{n} \tag{3}$$

where n_k represents the number of pixels with a light intensity equal to u_k, and n describes the number of pixels in the entire image. An enhancement technique for the histogram is CHE, in which the operator given in Eq.(2) can be described as [20]:

$$v_k = F(u_k) = \sum_{i=0}^{k} \left(\frac{n_i}{n}\right) \tag{4}$$

3. Proposed Algorithm

A modification of the classical histogram equalization technique is PLHE, of which the result is more effective and straightforward than that of the conventional version. For constructing a unified algorithm, the number of pixels related to a given light intensity n_k is normalized to produced $\tilde{n}_k$, which represents the normalized histogram as described in Eq. (5). A point processing model is generated by applying the thresholding process, which is implemented by replacing each component of the normalized histogram $\tilde{n}_k$ of an image with a step value ($Step_k$) of 0 if the component value $\tilde{n}_k$ is less than the binarization ratio B_r, or a step value of 1 if $\tilde{n}_k$ is greater than that constant. The running sum is evaluated and normalized to complete the point-processing model as given in Eqs. (6) and (7), respectively. The following steps are involved in the proposed algorithm:

ALGORITHM 1

STEP 1: Normalize the histogram as described by

$$\tilde{n}_k = \frac{n_k}{\max(n_k)}, k \in [0, L-1]. \quad (5)$$

STEP 2: Compare the number of pixels in the normalized histogram $\tilde{n}_k$ with the binarization ratio B_r,

IF $\tilde{n}_k < B_r$ **THEN**

$Step_k = 0$

ELSE

$Step_k = 1.$

ENDIF

STEP 3: Evaluate the running sum as expressed by

$$v_k = \sum_{i=0}^{k} Step_i. \quad (6)$$

STEP 4: Normalize the result of step 3 as follows:

$$\tilde{v}_k = Round\left(L \times \frac{t_k}{\max(t)}\right). \quad (7)$$

Two numerical examples are presented in Tables 1 and 2. These examples clarify the proposed algorithm explained in Algorithm 1. In these examples, we provide eight gray-level images, and a number of pixels for each gray level is listed in the n_k column. The B_rs of these examples are 10% and 50%.

Table 1. Example 1 with $B_r = 0.1$.

r_k	n_k	$\tilde{n}_k$	$Step_k$	v_k	$\tilde{v}_k$
0	40	0.2	1	1	1
1	200	1.00	1	2	2
2	30	0.15	1	3	3
3	10	0.05	0	3	3
4	90	0.45	1	4	4
5	100	0.50	1	5	5
6	120	0.60	1	6	6
7	90	0.45	1	7	7

Table 2. Example 2 with $B_r = 0.5$.

r_k	n_k	$\tilde{n}_k$	$Step_k$	v_k	$\tilde{v}_k$
0	40	0.2	0	0	0
1	200	1.00	1	1	2
2	30	0.15	0	1	2
3	10	0.05	0	1	2
4	90	0.45	0	1	2
5	100	0.50	1	2	5
6	120	0.60	1	3	7
7	90	0.45	0	3	7

As listed in Tables 1 and 2, the point-processing model $\tilde{v}_k$ of the proposed algorithm (Algorithm 1), which is produced for a small value of the binarization ratio B_r ($B_r = 0.1$) has a larger component value corresponding to each gray level u_k as compared to that produced for a larger value of B_r, i.e., the contrast stretching is increased as the value of the binarization ratio is reduced.

4. Experimental Results

The CHE and PLHE methods are implemented in MATLAB version 9.4. A set of four MRI images is selected to test the applied methods [21]. The results are shown in Figs. 2-13.

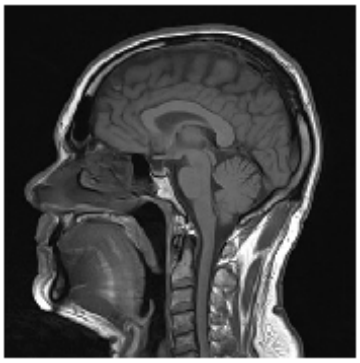

(a) Original MRI image.

(b) CHE.

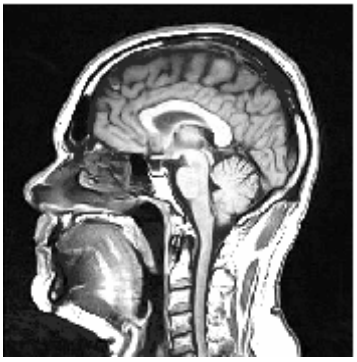

(c) PLHE.

Fig. 2. Result of the tested methods applied to MRI image 1.

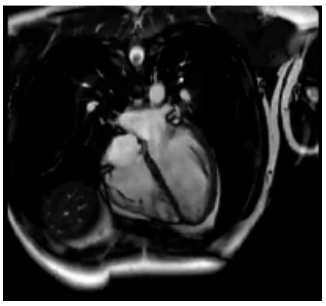

(a) Original MRI image.

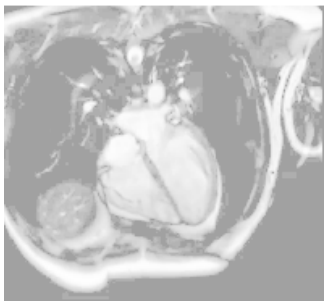

(b) CHE.

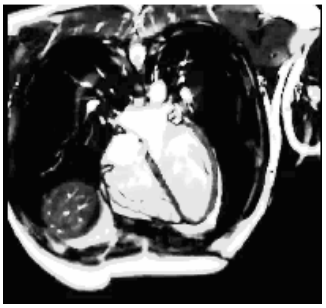

(c) PLHE.

Fig. 3. Result of the tested methods applied to MRI image 2.

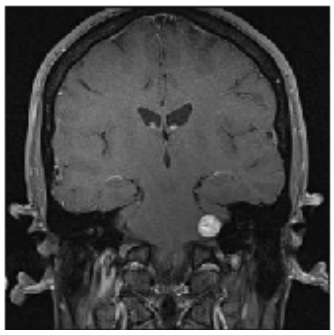

(a) Original MRI image.

(b) CHE.

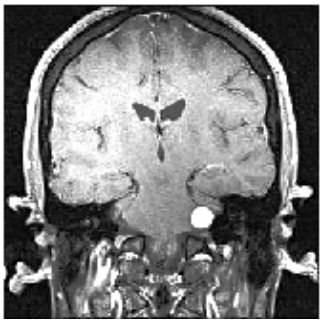

(c) PLHE.

Fig. 4. Result of the tested methods applied to MRI image 3.

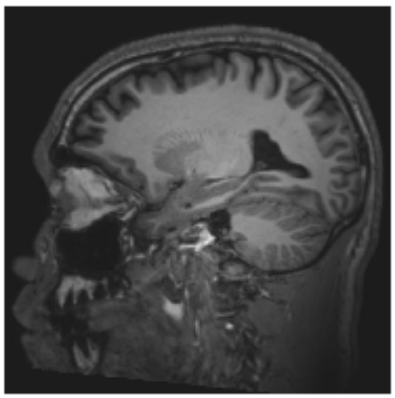

(a) Original MRI image.

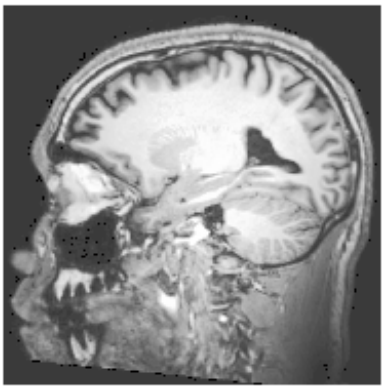

(b) CHE.

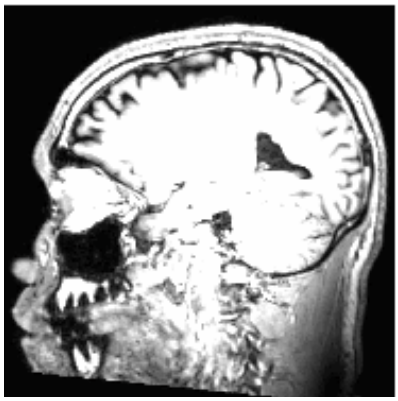

(c) PLHE.

Fig. 5. Result of the tested methods applied to MRI image 4.

As illustrates in Figs. 2(c)-5(c), Applying the PLHE algorithm (with $B_r = 0.035, 0.002, 0.11, 0.035$, respectively) provided visually satisfying results with no artifacts as compared to images resulted from applying CHE algorithm due to of extreme compensation of the light level intensities in the case of CHE algorithm (see Figs. 2(b)-5(b)).

Figures 6-9 show the histogram of the images shown previously in Figs. 2-5, respectively. The histogram plots shown in Figures 6(a)-9(a) reflect the large dark backgrounds in the corresponding images. This is well noticed in Fig. 7 (a). The effectiveness of the PLHE algorithm is reflected in terms of uniformly spread of the histogram components over grayscale range (see Figs. 6(c)-9(c)) as compared to the results of the CHE algorithm. As shown in Figs. 6(b) and 7(b), the gray levels move to bright levels, thereby providing increased lighting to the image while reducing the gray-level distribution. The gray levels are distributed evenly across the intensity range, as indicated in Figs. 6(c) and 7(c). The MRI image is shown in Fig. 3(a) has the least light content among all images in the image set, and this characteristic is evident in Fig. 7(b). A small B_r value is needed to enhance such images.

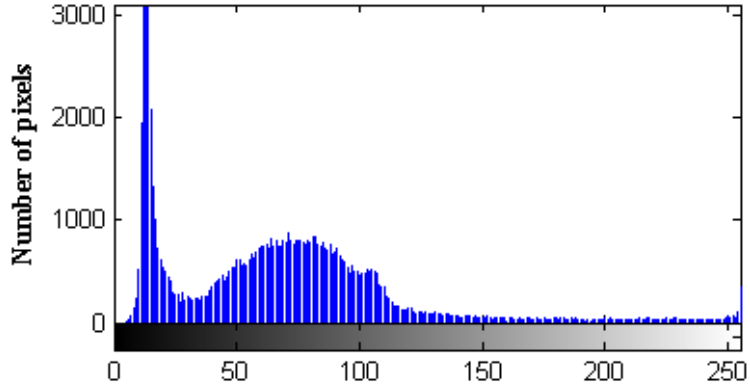

(a) Original MRI image.

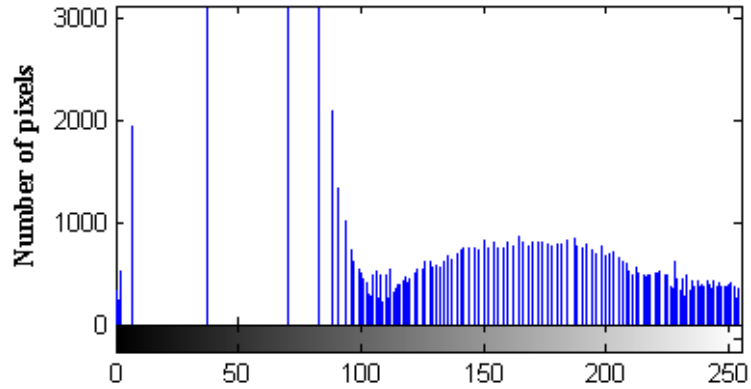

(b) Result of CHE.

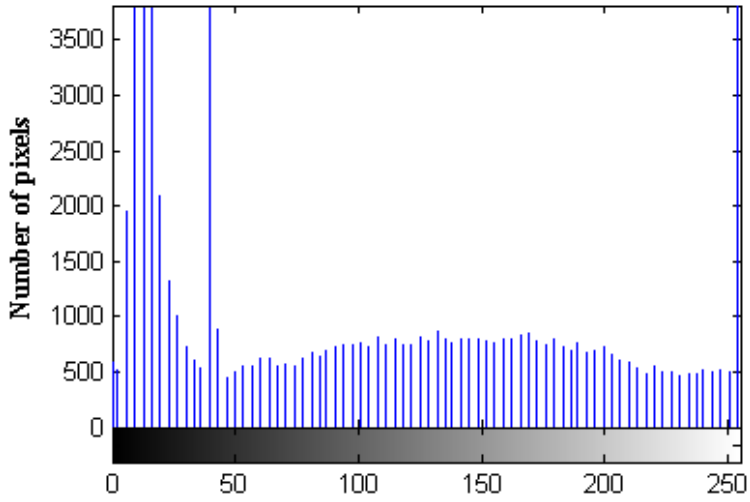

(c) Result of PLHE.

Fig. 6. Image histogram of MRI image 1.

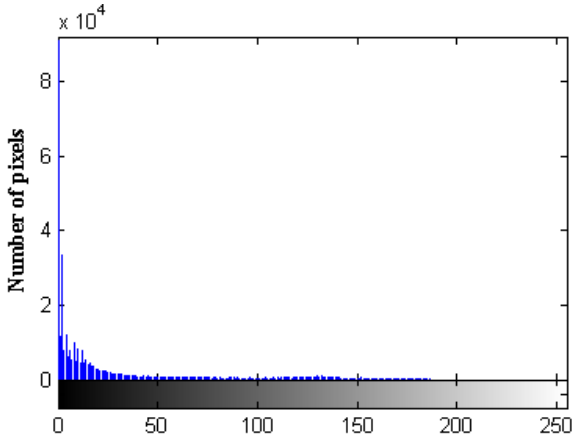

(a) Original MRI image.

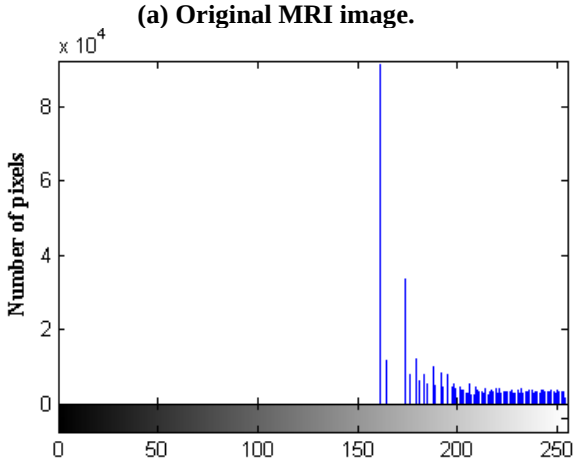

(b) Result of CHE.

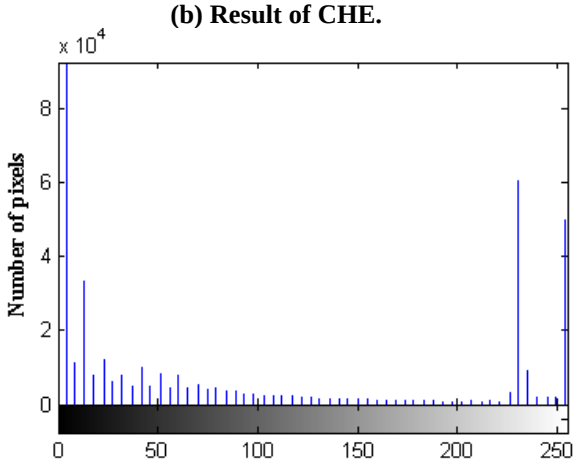

(c) Result of PLHE.

Fig. 7. Image histogram of MRI image 2.

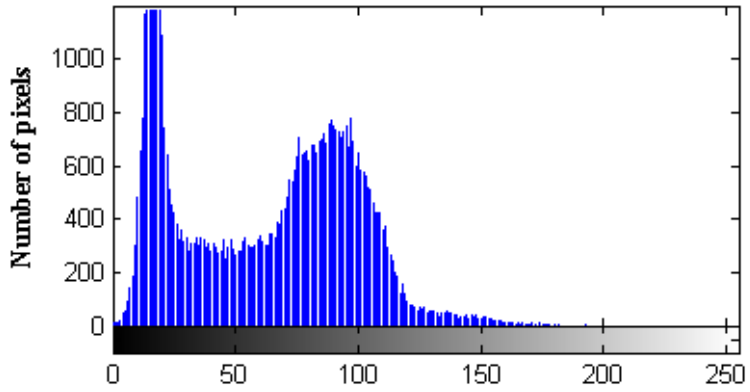

(a) Original MRI image.

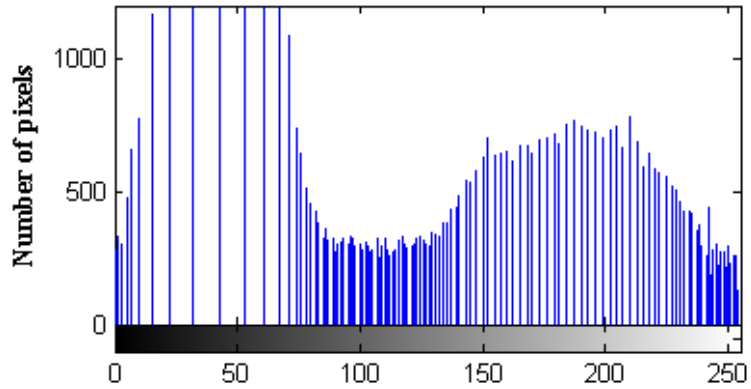

(b) Result of CHE.

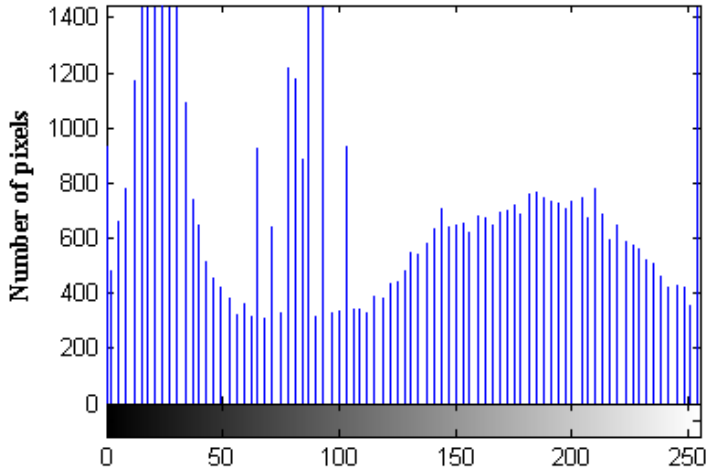

(c) Result of PLHE.

Fig. 8. Image histogram of MRI image 3.

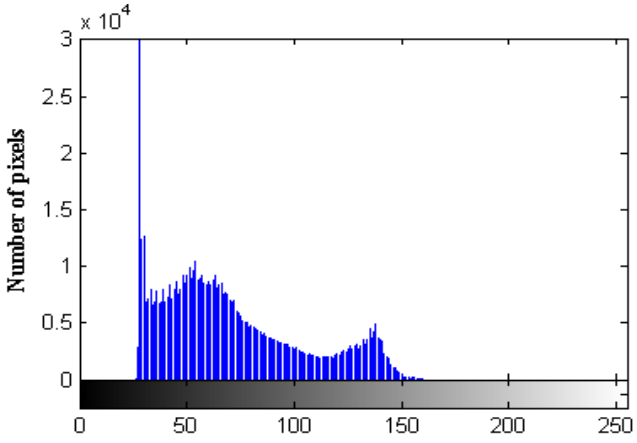

(a) Original MRI image.

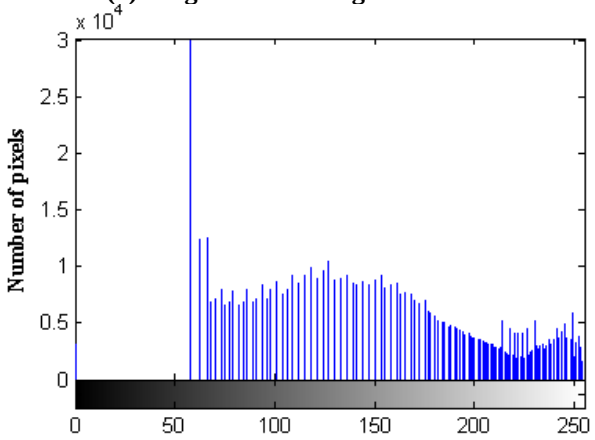

(b) Result of CHE.

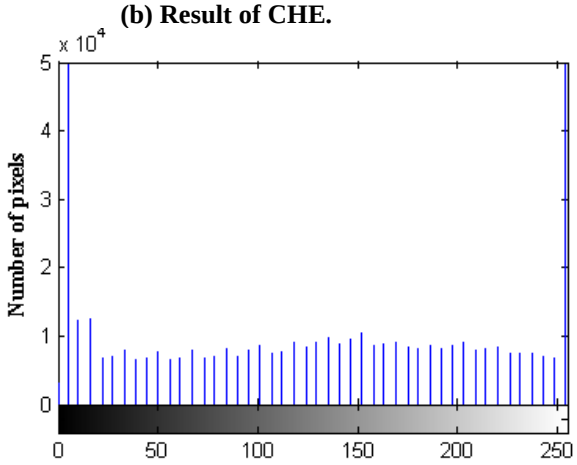

(c) Result of PLHE.

Fig. 9. Image histogram of MRI image 4.

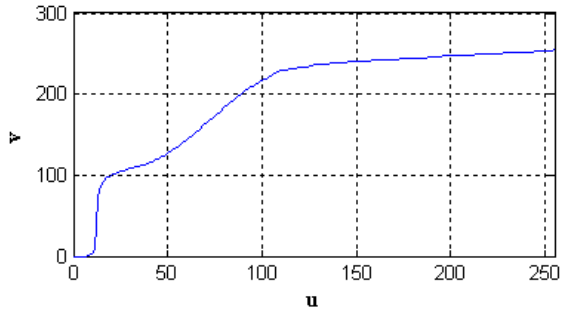

(a) CHE.

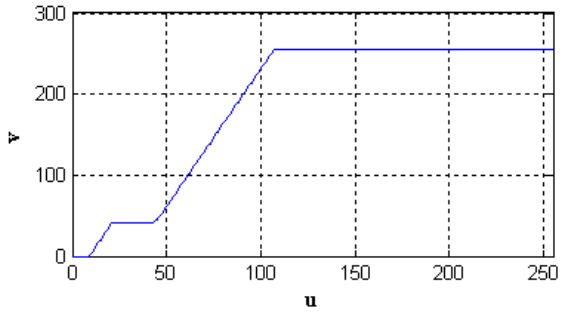

(b) PLHE.

Fig. 10. The transformation function applied to image 1.

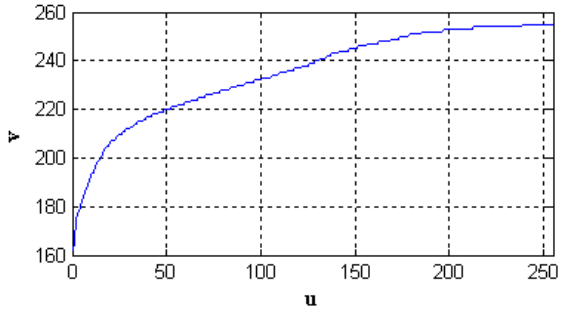

(a) CHE.

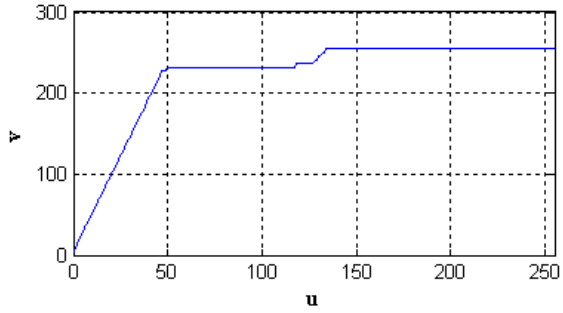

(b) PLHE.

Fig. 11. Transformation function applied to image 2.

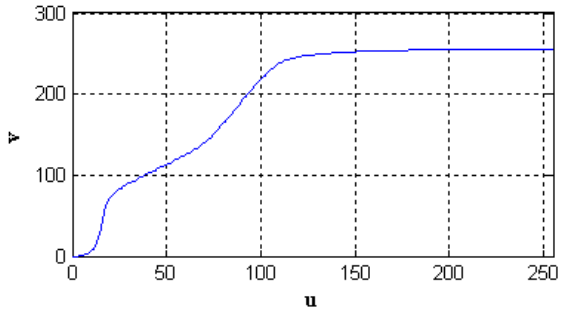

(a) CHE.

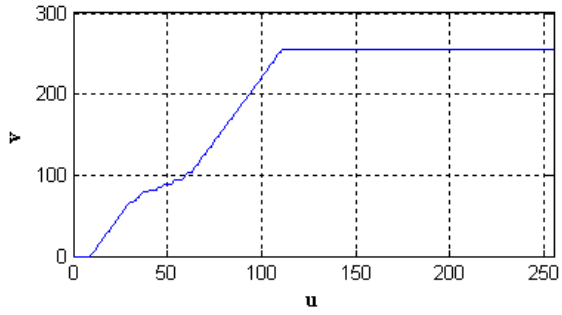

(b) PLHE.

Fig. 12. Transformation function applied to image 3.

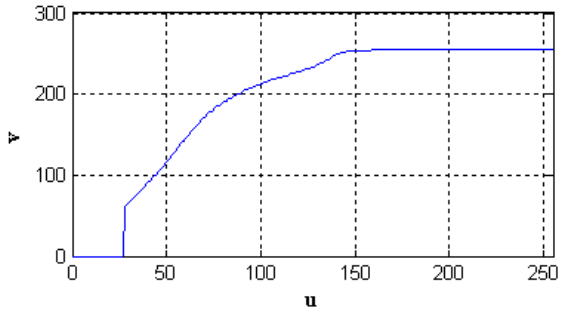

(a) CHE.

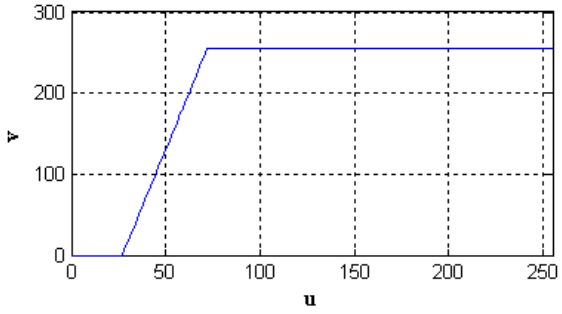

(b) PLHE.

Fig. 13. Transformation function applied to image 4.

The linearity shaped transformation function is shown in Figs. 10(b)-13(b) as compared to nonlinear transformation function Figs. 10(a)-13(a).

Two quantitative measures are selected to qualify the proposed enhancement method (refer to Table 3). The first measure is the entropy of the gray levels in an image. If the gray levels of an image have different values of frequencies, then the image has high entropy. If a flat histogram exists, then the image has low entropy [22]. The entropy H is expressed as:

$$H\big(p(u_k)\big) = -\sum p(u_k) \cdot \log_2\big(p(u_k)\big). \tag{8}$$

The second proposed measure reflects the edge enhancement or apparent sharpness in an image [23]. For this purpose, the edge is first evaluated using Sobel algorithm, which is implemented based on convolution kernels shown in Fig. 14.

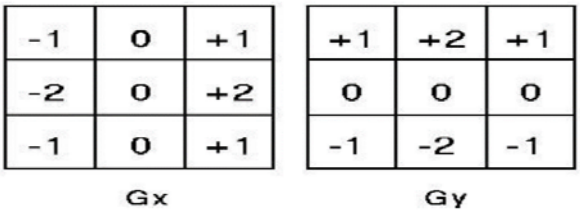

Fig. 14. Sobel kernels [24].

The gradients G_x and G_y result from convolving the kernels presented in Fig. 2 with the enhanced image. Both gradients are combined to obtain the following gradient magnitude:

$$|G| = \sqrt{G_x^2 + G_y^2} \tag{9}$$

The edge enhancement index (EHI) is expressed as

$$EHI = \sum\sum G^2 \tag{10}$$

Table 3. Quantitative measurement results.

Image Number	Image	H	EHI
Image 1	Original image	6.3658	3791
	Result of CHE	6.0959	4070
	Result of PLHE ($B_r = 0.035$)	5.2001	5040
Image 2	Original image	3.45371	21985
	Result of CHE	3.0788	29159
	Result of PLHE ($B_r = 0.002$)	2.6444	18347
Image 3	Original image	6.7192	2798
	Result of CHE	6.5920	2666
	Result of PLHE ($B_r = 0.11$)	6.0465	2909
Image 4	Original image	6.0129	16304
	Result of CHE	5.9255	19144
	Result of PLHE ($B_r = 0.035$)	3.9973	19662

The performance measures, which are listed in Table 3, show a reduction in the value of entropy for the images processed by the PLHE method. In the same manner, the EHI increases, thereby reflecting the sharpness of the resulting image.

5. Conclusion

This paper presented a new enhancement algorithm applied to medical applications. This algorithm is suggested to overcome the abnormal enhancement and unwanted artifacts that are introduced by the conventional enhanced algorithm. The fundamental concept of the PLHE is the thresholding step of the input histogram, which produces a suitable transform function. This function allows a high-level intensity and maximum detail maintenance. Moreover, the proposed algorithm simplifies the base algorithm by making it piecewise linear. The only limitation of the proposed algorithm is the extra factor B_r , which does not exist in the CHE algorithm and need to be selected to a suitable value to control the enhancement process. The B_r should be low if the contrast is low. The extension of the suggested algorithm to deal with other types of medical images, which is subject to our future work.

Nomenclatures

B_r	Binarization ratio
G_x	Gradient in the x direction
G_y	Gradient in the y direction
$\tilde{n}_k$	Normalize the histogram
$p(.)$	Probability
$T(.)$	Transformation function
u_k	Gray level
B_r	Binarization ratio
G_x	Gradient in the x direction
G_y	Gradient in the y direction
$\tilde{n}_k$	Normalize the histogram

Abbreviations

CHE	Conventional Histogram Equalization
EHI	Edge Enhancement Index
H	Entropy
PLHE	Piecewise Linear Histogram Equalization

References

1. Arun, A.S.; Mohamed, N.S.; and Prabakaran, D. (2013). Review of various image contrast enhancement techniques. *International Journal of Advanced Research in Computer Science and Software Engineering*, 2(11), 473-480.
2. El-Gamal, Z.A.; Elmogy, M.; and Atwan, A. (2016). Current trends in medical image registration and fusion. *Egyptian Informatics Journal*, 17(1), 99-124.
3. Bendoumi, M.A.; He, M.; and Mei, S. (2014). Hyperspectral image resolution enhancement using high-resolution multispectral image based on spectral unmixing. *IEEE Transactions on Geoscience and Remote Sensing*, 52(10), 6574-6583.

4. Kim, D.; Park, J.; Jung, J.; Kim, T.; and Paik, J. (2014). Lens distortion correction and enhancement based on local self-similarity for high-quality consumer imaging systems. *IEEE Transactions on Consumer Electronics*, 60(1), 18-22.
5. Ravanelli, D.; Dal P.; Centonze, M.; Casagranda, G.; Marini, M.; Del G.M.; and Valentini, A. (2014). A novel skeleton based quantification and 3-D volumetric visualization of left atrium fibrosis using late gadolinium enhancement magnetic resonance imaging. *IEEE Transactions on Medical Imaging*, 33(2), 566-576.
6. Amiot, C.; Girard, C.; Chanussot, J.; Pescatore, J.; and Desvignes, M. (2015). Curvelet based contrast enhancement in fluoroscopic sequences. *IEEE Transactions on Medical Imaging*, 34(1), 137-147.
7. Fu, X.; Wang, J.; Zeng, D.; Huang, Y.; and Ding, X. (2015). Remote sensing image enhancement using regularized-histogram equalization and DCT. *IEEE Geoscience and Remote Sensing Letters*, 12(11), 2301-2305.
8. Fan, W.; Wang, K.; Cayre, F.; and Xiong, Z. (2015). Median filtered image quality enhancement and anti-forensics via variational deconvolution. *IEEE Transactions on Information Forensics and Security*, 10(5), 1076-1091.
9. He, H.; Mandal, S.; Buehler, A.; Dean-Ben, X.L.; Razansky, D.; and Ntziachristos, V. (2016). Improving optoacoustic image quality via geometric pixel super-resolution approach. *IEEE Transactions on Medical Imaging*, 35(3), 812-818.
10. Mandal, S.; Dean-Ben, X.L.; and Razansky, D. (2016). Visual quality enhancement in optoacoustic tomography using active contour segmentation priors. *IEEE Transactions on Medical Imaging*, 35(10), 2209-2217.
11. Niu, Y.; Wu, X.; and Shi, G. (2016). Image enhancement by entropy maximization and quantization resolution upconversion. *IEEE Transactions on Image Processing*, 25(10), 4815-4828.
12. Ozan, O.; Enzo, F.; Konstantinos, K.; Mattias, H.; Wenjia, B.; Jose, C.; Stuart, A.C.; Antonio, M.; Timothy D.; Declan, P. O.; Bernhard, K.; Ben, G.; and Rueckert, D. (2018). Anatomically constrained neural networks (ACNNS): Application to cardiac image enhancement and segmentation. *IEEE Transactions on Medical Imaging*, 37(2), 379-383.
13. Long, M.; Li, Z.; Xie, X.; Li, G.; and Wang, Z. (2018). Adaptive image enhancement based on guide image and fraction-power transformation for wireless capsule endoscopy. *IEEE Transactions on Biomedical Circuits and Systems*, 12(5), 993-1003.
14. Yousif, A.S.; Sheikh, U.U.; and Omar, Z. (2019). A novel enhancement method for medical image using double density wavelet and stationary wavelet transforms. *Proceedings of the 9th International Conference on System Engineering and Technology (ICSET).* Shah Alam, Malaysia, 292-297.
15. Qiu, T.; Wen, C.; Xie, K.; Wen, F.Q.; Sheng, G. Q.; and Tang, X. G. (2019). Efficient medical image enhancement based on CNN-FBB model. *IET Image Processing*, 13(10), 1736-1744.
16. Yadav, A.; and Yadav, P. (2009). *Digital image processing*. Laxmi Publications Pvt Limited.

17. Firoz, R.; Ali, S.; Khan, M.N., and Hossain, K. (2016). Medical image enhancement using morphological transformation. *Journal of Data Analysis and Information Processing*, 4(1), 1-12.
18. Krieger, E.; Asari, V.K.; and Arigela, S. (2014). Color image enhancement of low-resolution images captured in extreme lighting conditions. *International Society for Optics and Photonics*, 9120, 1(9).
19. Jayaraman, K.B.; Esakkirajan, S.; and Veerakumar, T. (2011). *Digital image processing*. New Delhi: Tata McGraw Hill Education.
20. Burger, W.; and Burge, M.J. (2012). *Digital image processing: An algorithmic introduction using Java*. London: Springer.
21. Hornak, J.P. (2019). *The basics of MRI*. Rochester Institute of Technology.
22. Schneidewind, J.; Sips, M.; and Keim, D.A. (2006). Pixnostics: Towards measuring the value of visualization. *Proceedings of the IEEE Symposium on Visual Analytics Science and Technology*. Baltimore, USA, 199-206.
23. Brookshear, J.G. (2016). *Computer science: An overview* (10th ed.). Addison Wesley.
24. Shrivakshan, G.T.; and Chandrasekar, D.C. (2012). A comparison of various edge detection techniques used in image processing. *International Journal of Computer Science Issues*, 9(5), 269-276.